

FEATURE ARTICLE

Quadrupolar Solvent Effects on Solvation and Reactivity of Solutes Dissolved in Supercritical CO₂

John F. Kauffman*

Department of Chemistry, University of Missouri, Columbia, Missouri 65211-7600

Received: December 1, 2000; In Final Form: January 24, 2001

This article presents an overview of our recent studies of solvation and unimolecular reactivity in liquids and supercritical fluids. We review our research on rotational diffusion and photoisomerization kinetics of diphenylpolyenes in polar liquids and supercritical fluids. These results provide a qualitative demonstration of the influence of solvent quadrupole–solute dipole interactions on chemical reactivity in supercritical CO₂. The CO₂ quadrupole moment both increases solvent–solute friction experienced by a dipolar diphenylpolyene solute molecule and diminishes the activation barrier of the isomerization reaction via interaction with the polar transition state. We also review our recent studies of quadrupolar solvation and excited-state excimer formation kinetics of ADMA (1-[9-anthryl]-3-[4-*N,N*-dimethylaniline] propane). The ADMA studies have yielded quantitative confirmation of the importance of quadrupolar solvent–dipolar solute interactions in solvation and reactivity in supercritical CO₂. The results of these studies allow us to measure the contribution of solvent quadrupole–solute dipole interaction to the solvation energy of the excited-state charge transfer form of ADMA. We also discuss recent evidence indicating that the CO₂ quadrupole moment influences the kinetics of the charge-transfer reaction.

I. Introduction

Over the past 15 years, supercritical fluids (SCFs) have been applied to a variety of chemical processes such as solid-phase extraction, coating application, and chemical synthesis and analysis.^{1–3} Development of these applications have been largely motivated by a demand for environmentally friendly chemical processing, and as a result supercritical CO₂ has been a particularly important fluid. Solute behavior in SCF solutions is complex owing to the heterogeneity of solvent density, and numerous studies of solvation and reactivity have been performed on these solutions in order to develop a detailed, fundamental understanding of this unique solvent environment. Our research in this area has focused on the influence of specific

solvent–solute interactions on solvation and reactivity in SCFs, with emphasis on supercritical CO₂. We initiated this study with the goal of studying well-characterized unimolecular reactions in a variety of supercritical solvents. Over the years, we have examined trans–cis photoisomerization reactions of diphenylpolyenes, twisted intramolecular charge-transfer reactions, and intramolecular exciplex formation reactions. Through these studies we have come to appreciate the importance of solvent quadrupole–solute dipole (*q*–*d*) interactions in CO₂, and this article presents an overview of the experimental work that has brought us to our current understanding of these interactions. It begins with a brief discussion of the issue of solvent clustering in SCF solvents, followed by a discussion of rotational diffusion and trans–cis photoisomerization of diphenylpolyenes in polar liquids and SCFs. Both solvent viscosity and solvent “polarity” influence chemical reactivity of diphenylpolyenes, but it turns

* To whom correspondence should be addressed. E-mail: kauffmanj@missouri.edu.

out that viscous influences are easier to characterize in these reactions than polarity effects. To examine the influence of solvent polarity on chemical reactivity more fully, we have recently made an extensive investigation of solvation and exciplex formation kinetics of ADMA (1-[9-anthryl]-3-[4-*N,N*-dimethylaniline] propane) in nonpolar and dipolar liquids, mixtures of nonpolar and dipolar liquids, quadrupolar liquids, and SCFs. The second half of this article will present a summary of our recent results on ADMA solvation and reactivity in complex solvents, with emphasis on the importance of q - d interactions in supercritical CO₂.

II. Past and Present Perspectives on Local Density Enhancement in SCF Solutions

Solvent density augmentation around solute molecules in SCF solvents has received considerable attention over the past decade. Our understanding of this phenomenon has advanced considerably during this time, and its influence on unimolecular reactions, spectroscopic observables, and diffusion-controlled bimolecular reactions has been recently reviewed.⁴⁻⁶ In 1986, Eckert and co-workers observed large negative solute partial molar volumes in the naphthalene-ethane system near the ethane critical density.⁷ They attributed this observation to extensive solvent density enhancement around solute molecules, a phenomenon that is often referred to in the literature as "clustering". Eckert and co-workers developed a thermodynamic formalism indicating that the local solvent density should scale with the solvent isothermal compressibility, a quantity that diverges at the critical point. This landmark work was followed by a wide range of spectroscopic investigations in which researchers studied chromophoric solute molecules dissolved in SCFs, thereby probing the spatial region immediately surrounding the solute, the so-called cybotactic region. These studies revealed unusual dependences of solvent sensitive spectroscopic properties on solvent density, often exhibiting unanticipated features near the critical density of the pure fluid.⁸⁻¹⁷ For example, deviations of density-dependent spectral peak shifts from linearity in the Onsager reaction field function resulted in plateaus slightly below the critical density of the fluid. This behavior was attributed to fluid clustering around the chromophoric solute molecule. The proximity of the plateaus to the critical density seemed to suggest that the phenomenon responsible for the observed behavior might scale with the solvent isothermal compressibility. In 1994, Chialvo and Cummings¹⁸ examined the relationship between spectroscopic and thermodynamic observables in SCF solutions by decomposing the solute partial molar volume (and other thermodynamic quantities) of supercritical solutions at infinite dilution into short range and long range contributions using the Ornstein-Zernike equation. Using integral equation methods, they demonstrated that the short-range interactions are responsible for only about 5% of the observed density dependence of the solute partial molar volume. Furthermore, they demonstrated that, although the long-range term made its maximum contribution (i.e., its most negative excursion) at the critical density, the short-range term made its maximum contribution at about half the critical density. These observations clarified the distinction between short-range behavior that influences spectroscopic observables and the long-range correlations that are responsible for critical phenomena.

Egorov et al.¹⁹ have recently demonstrated via molecular dynamics simulations that the plateaus observed in the density dependence of spectroscopic quantities may result from a crossover between two regimes of behavior. The density

dependence of the observable in the high-density regime reflects the fact that repulsive (i.e., packing) interactions govern solvent density around a solute molecule, whereas attractive interactions govern the solvent density in the low-density regime. The slope of the density dependence differs in these two regimes, with the low-density slope increasing as the solvent-solute interactions become more attractive. Thus, the plateaus, which typically occur slightly below the critical density, reflect the crossover from attractive to repulsive control of the local solvent structure. Kajimoto has presented a similar argument.⁴

Recent simulations by Tucker and co-workers^{5,20,21} offer a compelling explanation for density augmentation. Solvent mass has been shown to be distributed inhomogeneously in a compressible solvent, and solute molecules prefer regions of high solvent density. Thus, solute molecules do not necessarily experience a solvent environment that can be characterized by the average bulk fluid density. Ruckenstein and Shulgin have recently arrived at a similar conclusion.²² At the same time, theoretical studies of solvation in compressible fluids²³ and solvatochromism²⁴ demonstrate that solute observables that are often used to characterize local density enhancement are primarily sensitive to solvent molecules within a solute's first one or two solvation spheres. Thus, common measures of solvent density probe a highly localized solvent environment and do not necessarily reflect solvent "condensation" around the solute molecule. To complicate matters, Fayer and co-workers have recently interpreted their extensive experimental measurements of vibrational relaxation times and solvatochromic shifts of tungsten hexacarbonyl with a theory that does not require the explicit assumption of fluid clustering around the solute.²⁵⁻²⁷ Egorov and Skinner²⁸ and Goodyear and Tucker²⁹ have presented alternative analyses of these results based in part on molecular dynamics and Monte Carlo simulations of the fluid density, and both studies attribute density anomalies in the vibrational relaxation rate to local density augmentation. Thus, numerous issues concerning the length scale of solute induced density enhancement, the time scale of density fluctuations, and the influence of these factors on chemical reactivity and other experimental observables remain to be resolved.

III. Rotational Diffusion in SCFs and Polar Liquids

Our early research focused on a particular aspect of solvent clustering in SCF solvents that we felt had been largely overlooked. From the above discussion, it is clear that polar solute moieties that have the potential to increase the magnitude of attractive solvent-solute interactions will influence the magnitude of the local density augmentation experienced by the solute. Thus, one of our most important goals has been to examine the influence of solute polar functional groups on solvent clustering in SCF solutions. Rotational diffusion time measurements via fluorescence anisotropy have a particularly significant role to play in these studies. Most spectroscopic studies of fluid clustering have focused on solute solvatochromic shifts. Solvatochromic probes typically contain one or more polar functional groups that endow their solvatochromic properties. As a result, solvatochromic studies do not offer a method of controlling a key variable (the solute functional groups) without simultaneously altering the experimental observable. Rotational diffusion, on the other hand, can be measured for solutes with or without polar functional groups, in gases and liquids. The rotational diffusion time τ_r depends on the solvent viscosity η according to the expression³⁰

$$\tau_r = \frac{\eta(\rho_1)V_p}{kT} f_{\text{stick}} C(\rho_1) + \tau_0 \quad (1)$$

where the parameters that depend on the local density ρ_1 have been indicated explicitly. This modified form of the Stokes–Einstein–Debye (SED) equation includes two correction factors f_{stick} and C and one additional term τ_0 in addition to the parameters of the original expression V_p and η . V_p is the solute volume, f_{stick} is a shape factor that accounts for the approximately ellipsoidal shape of the probe molecule, and C is a boundary condition factor that characterizes the extent to which the solvent sticks to the probe molecule. τ_0 is the zero-viscosity rotation time, which we approximate as the free rotor correlation time³¹

$$\tau_0 = \frac{2\pi(I)}{9(kT)}^{1/2} \quad (2)$$

kT is the thermal energy and I is the moment of inertia, which for the diphenylpolyenes is taken as the largest of the three moments owing to the direction of the transition dipole within the inertial axis system. Oftentimes researchers omit the free rotor term in studies of rotational diffusion in liquids or when the probe volume is large, because in these circumstances it represents only a small correction to the SED expression. We have found that rotational diffusion times of diphenylpolyenes in SCFs are short enough that the inertial rotation accounts for a significant contribution and cannot be ignored.

The rationale behind the study of rotational diffusion times in SCF solvents rests in the dependence of the viscosity experienced by the probe molecule on the local density around the probe. Prior to our study Betts et al.³² suggested that substantial clustering of supercritical N_2O around PRODAN (6-propionyl-2-(dimethylamino)naphthalene) occurred at low density. This was followed by a second paper that indicated a similar phenomenon around BTBP (*N,N'*-bis(2,5-*tert*-butylphenyl)-3,4,9,10-parylene-carboxodiimide) dissolved in several fluids.³³

Our studies of all-*trans*-diphenylbutadiene (DPB) and *trans*-(4-methanol)stilbene (HMS) in supercritical CO_2 contradicted these results.³⁰ Figure 1 shows a plot of the rotational correlation times of DPB and HMS in SCF CO_2 and HMS in SCF ethane plotted against reduced fluid density. We observed a monotonic increase in τ_r as the density was increased. On the basis of previous results,^{32,33} we anticipated substantially increased rotational diffusion times near the critical density, but the observed rotational diffusion times of both probes were very nearly equal to the free rotor times at these densities. This result does not support the hypothesis that nearly liquidlike densities are experienced by solute molecules dissolved in compressible solvents. Although Figure 1 does not exhibit unusual behavior at the critical density, it does reveal a stark contrast between the behavior of HMS and DPB at higher densities. Our original work analyzed this effect by interpreting eq 1 with a fluid clustering approach. We allowed the local density to exceed the bulk fluid density by a variable “density augmentation factor” and calculated density-dependent rotational correlation times using eq 1. By comparing measured density-dependent rotational diffusion times versus the predicted density dependence of this observable, we concluded that, although DPB appears to experience no local density augmentation, HMS experiences an environment that exceeds the bulk density by about 40% across most of the compressible regime. When a density of about 0.7 g/cm³ is achieved, the density augmentation factor begins to diminish. We attributed the difference between HMS and DPB to the HMS hydroxyl group and suggested that CO_2 –OH interactions appear to encourage fluid clustering.

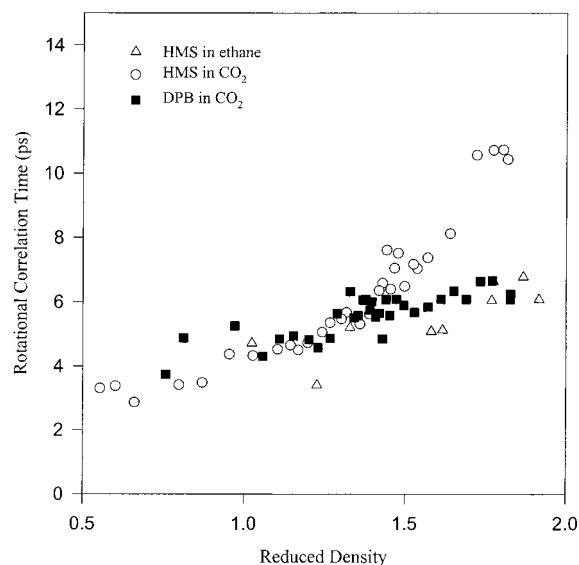


Figure 1. Rotational correlation times of DPB in SCF CO_2 (filled squares), HMS in SCF CO_2 (open circles), and HMS in SCF ethane (open triangles) plotted against reduced density. The reduced temperature is 1.01 ($\sim 34^\circ C$) for all systems.

Heitz and Maroncelli (HM) have recently observed a monotonic increase in the rotational diffusion times of several solutes dissolved in supercritical CO_2 , without excessive variations in the low-density regime, thus corroborating one of our observations.³⁴ However their approach to analysis of the data differs markedly from ours. They have compared the SCF results with measurements in a variety of liquids and utilize the entire body of data for a particular solute to characterize the dependence of the observed boundary condition factor C on the solvent. They use “normal” hydrodynamic behavior characterized by the SED equation as the reference behavior against which rotational diffusion in SCFs is measured. In the case of BTBP, the boundary condition factor is essentially unity (indicating stick boundary condition) across the entire range of η/T , including the low viscosity regime in which CO_2 has been investigated. This contrasts the behavior of another solute, bis(phenylethynyl)-anthracene (PEA), which exhibits a variable boundary condition factor. They interpret the behavior observed in supercritical CO_2 as arising from density augmentation of the fluid around PEA. Furthermore, they have applied their method of analysis to our results on HMS and DPB and draw conclusions that contradict ours. Their analysis suggests that substantial variation in the boundary condition may occur for DPB dissolved in supercritical CO_2 , which they do not observe in the limited HMS data that is currently available. However, although the boundary condition factor of HMS in supercritical CO_2 does not vary with density, it is larger than that of DPB in CO_2 . They also emphasize the difficulty of characterizing local density quantitatively on the basis of rotational diffusion times because of the challenges that still remain in the interpretation of this phenomenon under conditions encountered in such studies. For example, solute size in relation to the solvent size is a well-known influence on the boundary condition factor.³⁵

One important difference between our analysis and the HM analysis is that we explicitly recognize a finite zero-viscosity intercept in our analysis, and this affects the magnitude of the boundary condition factor that is calculated from the experimental data. By first subtracting τ_0 from τ_r and applying HM analysis to our experimental data, we have concluded that the boundary condition factor of DPB in CO_2 is constant across the density range examined in our study, whereas the boundary

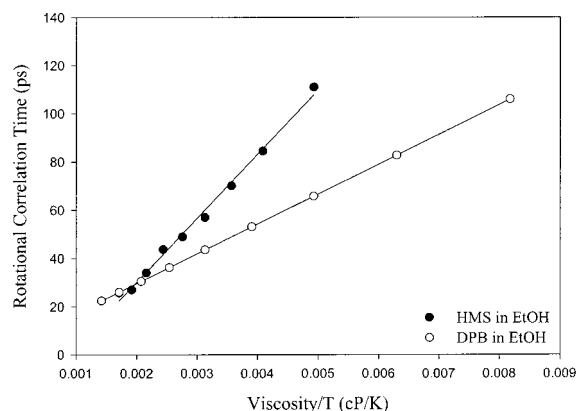


Figure 2. Rotational correlation times of DPB and HMS in liquid ethanol. HMS has longer rotational correlation times in all liquid alcohols. This effect has been attributed to strong interactions between solvent and solute (from ref 37).

condition factor of HMS increases by nearly a factor of 4 upon increasing density in CO₂ from the compressible regime to liquid density. We also note that attributing all variation to changes in the boundary condition factor overlooks the importance of solvent density in determining the local solvent viscosity. These considerations demonstrate the difficulty of arriving at a precise measure of local solvent density from experimental rotational correlation time data. On the other hand, we can derive some qualitative conclusions from comparative studies. A comparison of HMS and DPB in supercritical CO₂ demonstrates the influence of a polar functional group on solvent–solute friction. A comparison of HMS in supercritical ethane and CO₂ (Figure 1) emphasizes the specificity of the polar solute interaction with CO₂.³⁶ Interestingly, the HMS–ethane results exhibit the same modest increase with increasing density that we have observed in the DPB–CO₂ system. Because the solvent and solute sizes of these systems are very similar, this result is consistent with “normal” hydrodynamic theory. The HMS–CO₂ data therefore reflects a deviation from normal behavior that we have attributed to q–d interactions between the CO₂ solvent quadrupole and the HMS solute dipole.

To examine the influence of the solute hydroxyl group on rotational diffusion times over a broader range of conditions, we have recently compared solvent- and temperature-dependent rotational diffusion times of HMS and DPB in a series of *n*-alcohols.³⁷ We have found that in all cases HMS exhibits longer rotational correlation times than DPB, as illustrated in Figure 2. In accordance with the modified SED equation, HMS and DPB should experience nearly identical hydrodynamic friction because they are nearly identical in shape and size. The observed difference can be interpreted as a difference in the boundary condition factor, with HMS exhibiting a larger boundary condition factor in all solvents across the entire range of temperatures. Note that this interpretation is consistent with Heitz’s suggestion that HMS has a larger boundary condition factor in SCF CO₂. This result emphasized the fact that HMS interacts more strongly than DPB with both alcohols and CO₂, whereas it behaves similarly to DPB in alkanes such as hexane and supercritical ethane. We have analyzed the alcohol results using the Nee–Zwanzig theory of dielectric friction, which computes the value of an additive contribution to the rotational diffusion time resulting from the interaction of a solute dipole with a continuum dielectric solvent characterized by a dielectric constant.³⁸ Our analysis has suggested that hydrogen bonding between solvent and solute may be the source of strong interactions between solvent and solute, a result that is not

unexpected. Other groups^{39,40} have also shown that rotational diffusion is strongly influenced by attractive solvent–solute interactions. Several improvements to Nee–Zwanzig theory have been presented,^{41,42} but they all exhibit the same dependence on static solvent dielectric properties and solute dipole moment. All theories of dielectric friction reflect the influence of dipole solvent–dipole solute interactions on rotational diffusion. This method of analysis fails for the HMS CO₂ system because the solvent dielectric constant does not vary significantly as density is increased. This has led us to conclude that q–d interactions are at play in this system.

The presumed additivity of the hydrodynamic and dielectric contributions to solvent–solute friction is predicated on the separability of the contributions of attractive and repulsive torques to the friction coefficient. Several recent publications indicate that this separation is often a poor approximation, particularly when strong attractive interactions between solvent and solute are operative. Kumar and Maroncelli⁴³ and Kurnikova et al.^{44,45} have both demonstrated through molecular dynamics simulations that electrostatic solvent–solute interactions contribute to the hydrodynamic friction as the result of interaction-induced “electrostriction” of solvent around solute. Thus, an attractive solvent–solute interaction influences the repulsive hydrodynamic contribution to solvent–solute friction. Electrostriction is currently not addressed in fundamental theories of rotational dynamics in solution, and therefore, it cannot be properly examined in experimental studies. Qualitatively, electrostriction is tantamount to local density augmentation and offers a compelling explanation for the behavior of HMS dissolved in SCF CO₂. The solvent friction experienced by HMS in CO₂ that is in excess of the “normal hydrodynamic” behavior characterized by DPB in CO₂ (see Figure 1) may result from strong attractive interactions between CO₂ and the HMS hydroxyl group, amplified by electrostrictive local density augmentation. Once again we emphasize that the lowest order electrostatic interaction responsible for HMS–CO₂ attraction is a solute dipole–solvent quadrupole interaction.

IV. Diphenylpolyene Photoisomerization and Solvent Polarity

DPB and HMS belong to the family of diphenylpolyenes that are known to undergo trans–cis isomerization in the excited electronic state. The kinetics of DPB photoisomerization have been widely studied over the past 30 years,^{46–54} whereas HMS has only recently been investigated.^{30,36,37,55} The isomerization reaction is known to depend on the viscosity of the medium in which the solute is dissolved. The viscosity dependence of the isomerization reaction has been investigated within the context of Kramers theory.^{49,51,56,57} This theory casts the rate constant in the following form

$$k_{\text{nr}} = \frac{\omega_a \xi}{4\pi\omega_b} \left\{ \left[1 + \left(\frac{2\omega_b}{\xi} \right)^2 \right]^{1/2} - 1 \right\} \exp\left(\frac{-E_a}{kT}\right) \quad (3)$$

where ω_a and ω_b are the initial well frequency and the imaginary barrier frequency, respectively, assuming a one-dimensional, piecewise parabolic potential-energy surface. (In reality, the potential-energy surface governing nuclear coordinates is multidimensional. The shape of the potential along the reaction coordinate may depend on the degree of excitation of nuclear modes orthogonal to the reaction coordinate, though such “multidimensional effects” are difficult to verify experimentally.) ξ is a solvent friction parameter given in units of frequency. Hydrodynamic theories relate ξ to the solvent viscosity, but

TABLE 1: Comparison of Isomerization Rate Constants for DPB in Supercritical CO₂^a

temperature (K)	density (g/cm ³)	$k_{\text{isom}}/10^9$ (Gehrke et al.)	$k_{\text{isom}}/10^9$ (our work)
305	0.7		1.49
308	0.7		1.58
313	0.7		1.66
318	0.7		1.75
323	0.7		1.88
328	0.7		2.02
332	0.76	2.13	
333	0.7		2.13
338	0.7		2.2
343	0.7		2.28
348	0.7		2.42
350	0.89	2.45	
350	1.1	2.39	
350	1.21	2.15	
350	1.31	1.87	
384	0.08	5	

^a The first two columns describe the conditions of the measurements. The third column presents isomerization rates from the transient absorption measurements of Gehrke et al.,⁵¹ and the fourth column presents our isomerization rates determined from fluorescence lifetimes.

hydrodynamics are not appropriate for fast unimolecular isomerizations in which a small reactive body undergoes primarily rotational motion over the course of the reaction. Lee et al.⁵⁸ have suggested that ξ be replaced by β , the angular velocity correlation frequency, when Kramers theory is applied to diphenylpolyene photoisomerization reactions. β is given by the Hubbard relation:⁵⁹

$$\beta = (6kT/I)\tau_r \quad (4)$$

where kT is the thermal energy, I is the solute moment of inertia, and τ_r is the solute rotational correlation time. Lee et al.⁵⁸ refer to this as the Kramers–Hubbard model. Note that the Kramers–Hubbard frequency factor can also be derived from Grote–Hynes theory⁶⁰ for barrier crossing in solution.⁵⁵ Kramers theory isolates the influence of solvent viscosity in the preexponential term. Schroeder⁵⁴ and Troe and co-workers^{51,53,61–63} have made extensive study of DPB and stilbene in a variety of compressed solvents including SCFs and liquid alcohols. They typically observe a decrease in the isomerization rate as the fluid density is increased. The dependence of the rate on solvent viscosity is very shallow in the gaslike solvent density range and becomes steeper as the density increases. Our isomerization rate data for DPB and HMS in CO₂ exhibits a similar trend. We have analyzed the combined lifetime and rotational diffusion results of HMS using the Kramers–Hubbard analysis for both CO₂ and hexane, and we arrive at an activation barrier of about 2 kcal/mol³⁶ and 4.6 kcal/mol, respectively. The barrier in CO₂ is substantially lower, even though CO₂ and hexane have similar dielectric constants. We have observed a similar barrier lowering in the activation barrier of DPB in CO₂ (2.3 kcal/mol) compared with hexane (4.7 kcal/mol,^{64,65}). Schroeder and Troe have observed a similar effect in comparative studies of stilbene in alkanes (~ 2 kcal/mol) and CO₂ (~ 1.6 kcal/mol) at high temperature.^{54,61} However, barrier lowering was not observed for DPB in compressible solvents, arriving at activation barriers of ~ 2.5 kcal/mol in both alkanes and CO₂.⁵⁴ We have compared our isomerization rates determined from fluorescence lifetime measurements of DPB in CO₂ alongside the results of Troe and co-workers⁵¹ from transient absorbance studies of the same system in Table 1. The comparison demonstrates remarkable agreement between the measurements as well as the activation

barriers derived from the CO₂ data. A comparison of our CO₂ data with other studies of DPB isomerization in dense alkanes^{64,65} suggests that CO₂ reduces the barrier to both HMS and DPB photoisomerization. The discrepancy between our conclusion and the conclusions of Troe and co-workers are puzzling. Schroeder⁵⁴ and Gehrke et al.⁵¹ have suggested that multidimensional influences on the potential-energy surface may result in a temperature-dependent barrier in DPB, and this may be responsible for the discrepancy between our results measured at relatively low temperatures and their results measured at significantly higher temperatures (i.e., the shape of the reaction coordinate depends on the degree of excitation of orthogonal coordinates and, thus, on temperature). We have attributed the barrier lowering observed in our data to the influence of CO₂'s quadrupole moment on the zwitterionic transition state of the isomerization reaction. This postulate is consistent with a series of studies of diphenylpolyene isomerization rates in alcohols that demonstrated that solvent permittivity influences the activation barrier of stilbene, DPB and HMS.^{49,55,66} Schroeder et al.⁶³ have arrived at a similar conclusion on the basis of pressure dependent studies of stilbene in alcohols.

The photoisomerization results along with the rotational correlation time studies of diphenylpolyenes provide some insight into solvation and reactivity in SCF solvents. Clearly solvent friction can play a central role in governing chemical reactivity in SCFs, as it often does in liquids. However, the body of evidence does not appear to implicate solvent clustering as a general mechanism for controlling chemical reactivity in supercritical solvents. Strong solvent–solute friction in the HMS–CO₂ system appears to be the result of strong interactions between a particular solvent, CO₂, and a particular functional group on the solute, the hydroxyl group on HMS. Furthermore, this effect is weak at low CO₂ density where solvent clustering is expected to be most important. The apparent absence of excess friction resulting from solvent clustering around reactants in bimolecular reactive systems has also been observed by Brennecke and co-workers.^{6,67} Thus, solvent clustering around solute molecules in SCF solutions appears to have little influence on kinetics of viscosity-controlled chemical reactions. On the other hand, our analysis of diphenylpolyene isomerization rates in supercritical CO₂ reflects the influence of the CO₂ quadrupole moment on the activation barrier, an effect that will be important regardless of the extent of fluid clustering. Theories of quadrupolar influences on chemical reactivity that can be easily applied to diphenylpolyenes are not currently available. Therefore, we have searched for other models of chemical reactivity in SCF environments that offer a more detailed view of this phenomenon. The remainder of this paper presents an overview of our recent investigations of another molecule that undergoes unimolecular isomerization in the excited electronic state, ADMA.

V. ADMA in Liquid and SCF Solvents

ADMA undergoes a charge-transfer reaction in the excited electronic state in both polar and nonpolar solvents. The kinetics of the unimolecular reaction have been extensively studied by Eisenthal and co-workers,^{68–70} and Mataga and co-workers.^{71–74} The nature of the charge-transfer state is similar to a bimolecular exciplex between electronically excited anthracene (A*) and dimethylaniline (DMA).⁷⁵ Upon excitation the anthracene moiety becomes an electron acceptor whose electron affinity is equal in magnitude to the oxidation potential of ground state anthracene (A; i.e., the acceptor level is the HOMO of A, because it is only partially filled after $\pi-\pi^*$ excitation to A*). As it turns out, the HOMO of the DMA (which derives

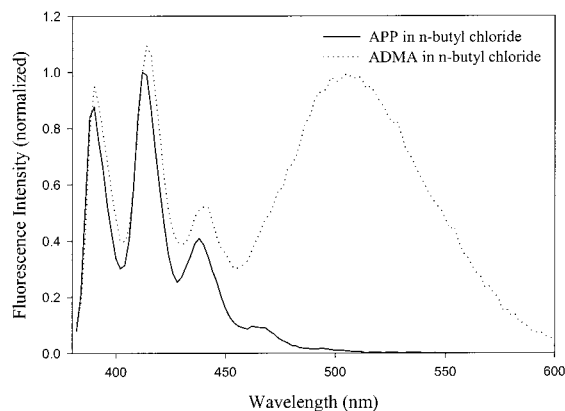


Figure 3. Spectra of ADMA and APP in *n*-butyl chloride. ADMA exhibits an additional band assigned to emission from a charge-transfer SH excited state.

significant character from the nonbonding nitrogen orbital) has a higher energy than the A* acceptor level. As a result, DMA can transfer an electron to A*. (The resulting exciplex has a delocalized negative charge on the anthracene moiety and a positive counter charge centered on the DMA nitrogen.) In both bimolecular and unimolecular cases, the charge transfer can only occur when the A and DMA moieties are in close proximity to one another, and the probability for electron transfer at a particular distance depends on the electrostatic properties (e.g., dielectric constant) of the solvent. In nonpolar solvents, the molecule must fold in order to bring the A* and DMA moieties close enough to one another for the charge transfer to occur, and as a result, the charge-transfer reaction is viscosity-dependent. Polar solvents support longer-range charge transfer, but in most cases (i.e., when $\epsilon < 20$), the resulting extended charge-separated species is drawn to the folded configuration by Coulombic attraction.^{72,73} In both cases, ADMA eventually assumes a sandwich-like charge-transfer configuration, and the resulting “sandwich heteroexcimer” (SH) is fluorescent. In contrast, the extended charge-transfer configuration, or “loose heteroexcimer” (LH) has a very low fluorescence quantum yield. Figure 3 exhibits two distinct contributions to the fluorescence spectrum of ADMA dissolved in tetrahydrofuran after excitation of the anthracene moiety at 387 nm.⁷⁶ Also shown is the spectrum of APP (1-(9-anthryl)-3-phenyl propane), a reference compound that does not undergo charge transfer. The emission at wavelengths below 450 nm resembles the anthracene spectrum and is observed in both ADMA and APP spectra. This region of the spectrum has been assigned to the emission from the nonpolar locally excited (LE) state of ADMA.⁷¹ The broad emission in the 450–600 nm range is only observed in the ADMA spectrum and has been assigned to emission from the SH.⁶⁸ These spectral features mimic those of the bimolecular anthracene–DMA complex.⁷⁵ A schematic energy level diagram showing kinetic pathways and their dependence on solvent polarity is shown in Figure 4. Because the LE state must attain the folded conformation before charge transfer occurs in nonpolar solvents, the rate of disappearance of reactant (characterized by the decay time of the time-resolved anthracene emission) is equal to the rate of formation of product (characterized by the rise time of the time-resolved charge-transfer state emission). Both of these observables exhibit a power law dependence on solvent viscosity in nonpolar solvents.^{70,77} In solvents of intermediate polarity ($\epsilon < 20$), the charge-transfer mechanism is more complicated and the disappearance and formation rates are not commensurate. In highly polar solvents, the LH configuration is the most stable charge-transfer confor-

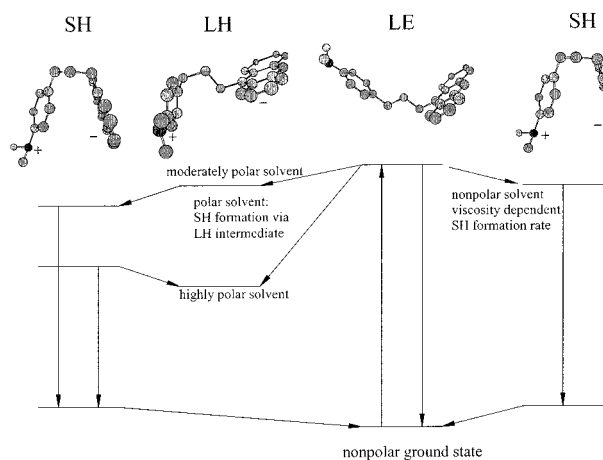


Figure 4. Energy level scheme that governs excited-state isomerization kinetics of ADMA. In nonpolar solvents, the mechanism for SH state formation is mediated by solvent viscosity. In polar solvents ($\epsilon > 10$), the favored pathway to the SH state is through the charge-separated LH intermediate. The weakly emissive LH state becomes the low energy configuration in highly polar solvents. New evidence indicates that the rate of the nonpolar mechanism is also mediated by solvent polarity in weakly polar solvents.

mation and the red shifted fluorescence is practically unobservable.^{69,73} Competition between the viscosity-controlled versus polarity-accelerated pathways is mediated by solvent polarity through its influence on the energy of the LH intermediate, as illustrated in Figure 4. Importantly, the nonpolar mechanism is characterized by a single-exponential decay of the anthracene emission, whereas a multiexponential decay is characteristic of the polar mechanism.^{73,74} Thus, the decay kinetics offers a useful, though untapped observable that characterizes the local environment of the ADMA molecule.

Recently we have used solvatochromic measurements of the ADMA SH emission in a variety of liquids, liquid mixtures, and SCF solvents to extract information concerning the local solvent environment. We have found that a broad range of solvatochromic effects can be understood within the context of continuum theories of solvation when these theories are properly applied. Furthermore, we have initiated a thorough examination of the kinetics of ADMA charge-transfer isomerization in complex environments, and we find that we can extract a great deal of information concerning the influence of the solvent environment on the kinetics of the reaction by utilizing both spectroscopic and kinetic data. The following sections summarize our most important results to date.

V.A. Spectroscopy of ADMA in Nonpolar, Dipolar, and Quadrupolar Fluids. Mataga demonstrated that the ADMA SH peak energy in dipolar solvents exhibits a linear dependence on the Lippert–Mataga solvent polarity function F given by

$$F = \frac{1}{4\pi\epsilon_0} \left(\frac{2(\epsilon - 1)}{2\epsilon + 1} - \frac{n^2 - 1}{2n^2 + 1} \right) \quad (5)$$

We have corroborated this study and have extended it to include a broad variety of solvents and solvent mixtures. In examining this phenomenon, it is useful to categorize solvents as dipolar and nondipolar.⁷⁸ Interactions between dipolar solvents and dipolar solutes are dominated by dipole–dipole interactions. Solvents that are typically considered polar exhibit relatively large dielectric constants as a result of permanent dipolar charge distributions within the molecules. Many solvents that are typically considered nonpolar can be categorized as a special class of dipolar solvents that only interact with polar solutes

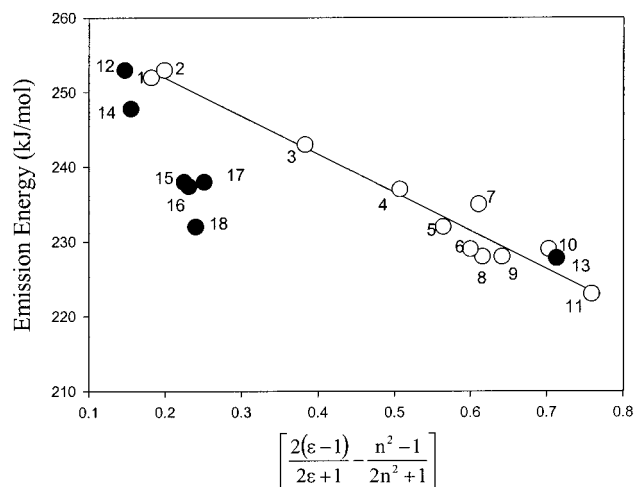


Figure 5. LM plot of the ADMA SH emission in pure solvents. Numbers in the plot match the solvents given in Table 2. The symbol sizes reflect the measurement uncertainty due to spectrometer resolution. Open circles are dipolar solvents, and filled circles are quadrupolar and supercritical solvents. The linear relationship with dipolar solvents indicates that solvent–solute interactions do not significantly distort the solute charge distribution in the SH configuration.

TABLE 2: ADMA Peak Energies in Various Solvents^a

solvent	SH peak (nm)	peak energy (kJ/mol)
hexane (1)	474.6	252
cyclohexane (2)	473.2	253
dibutyl ether (3)	492.3	243
diethyl ether (4)	504.2	237
<i>tert</i> -amylalcohol (5)	514.6	232
<i>n</i> -butyl chloride (7)	509.00	235
ethyl acetate (6)	522.6	229
tetrahydrofuran (8)	523.9	228
methylene chloride (9)	526.1	227
isoamyl alcohol (10)	522.9	229
ethanol (11)	537.1	223
supercritical ethylene (12)	473.4	253
supercritical fluorofrom (13)	525.3	228
supercritical CO ₂ (14)	483.9	248
benzene (15)	504.1	237
tetrafluorobenzene (16)	502.7	238
toluene (17)	502.0	238
1,4-dioxane (18)	516.3	232

^a Solvents 1–11 are dipolar, 12–14 are supercritical, and 12 and 14–18 are quadrupolar. The numbers in the solvent column indicate that appropriate data point in Figure 5.

via induced solvent dipole moments (i.e., polarizability). We can rephrase this categorization using the following functional definition. When the solvent dielectric constant characterizes the interaction between solvent and dipolar solute, the solvent is considered dipolar. (Of course, one must be careful to develop a correct functional dependence of the experimental observable on solvent dielectric constant, and this is seldom trivial.) Nondipolar solvents generally have very small dipole moments and therefore low dielectric constants but often exhibit solvatochromic polarities that exceed expectations. In other words, nondipolar solvents interact with dipolar solutes more strongly than their dielectric constants would suggest, and recently, such effects have been correlated with solvent quadrupole moments.^{78–82}

Figure 5 presents the peak energies of the ADMA SH emission measured in a variety of dipolar and quadrupolar solvents. Table 2 lists the solvents that contribute to this plot, which include alkanes, ethers, chlorinated solvents, and alcohols. The peak energy in dipolar (even hydrogen-bonding) solvents

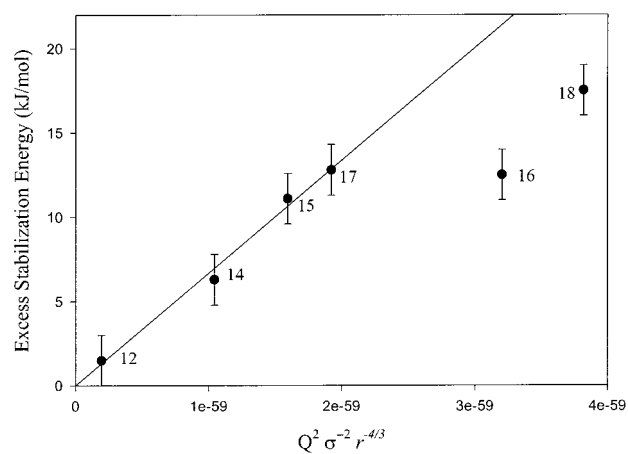


Figure 6. Excess solvation energy plotted against the density independent quadrupole function. The line is a linear regression fit of the solvents for which the effective axial approximation holds (from ref 86).

can be adequately described by the relationship^{71,76}

$$E_p \text{ (kJ/mol)} = -51.104[F] + 262 \quad (6)$$

The first term on the right is solvent dependent, and the second term represents the peak energy in a vacuum. The latter agrees well with the emission spectra of ADMA in supersonic jets.^{83,84} Because the heteroexcimer emission peak energies in dipolar solvents are reasonably linear in F , we surmise that the ground state dipole moment is approximately zero.⁸⁵ This is consistent with the small solvatochromic shift (approximately 2 nm when the solvent is changed from *n*-hexane to ethanol) observed in the ADMA absorbance spectrum. Analysis of the slope given in eq 6 indicates an excited-state dipole moment of ~ 12 D. The linear behavior observed in Figure 5 is expected for dipolar solvents because the Lippert–Mataga theory is based on the dipolar continuum model of solvation.⁸⁵ Thus, the Lippert–Mataga regression line offers a useful diagnostic of “normal” versus “unexpected” behavior.

Our most recent study of solvent influences on ADMA spectroscopy has been designed to probe solvatochromic effects resulting from interaction between the ADMA excited-state dipole and quadrupolar solvents. The nondipolar solvents exhibit a sizable deviation from the linear Lippert–Mataga prediction, indicating an excess stabilization over that predicted from dipole–dipole interactions. Because the ADMA peak energy characterizes its solvation energy, we have interpreted this deviation as an “excess solvation energy” because of solvation of the solute dipole by the quadrupole moment of the solvent. We have analyzed the solvation energy according to the Matyushov–Voth (MV) theory, a recently published theory of quadrupolar solvation. In accordance with this theory, the ratio of the quadrupolar solvation energy E_q to the dipolar solvation energy E_d is approximately equal to

$$\frac{E_q}{E_d} \approx 2.0 \frac{Q^2}{m^2 \sigma^2 r_{0s}^4} \quad (7)$$

where Q is the solvent quadrupole moment, m is the solvent dipole moment, $r_{0s} = R_0/\sigma + 0.5$, R_0 is the solute radius, and σ is the hard sphere diameter of the solvent. We are able to predict E_d for ADMA in any solvent on the basis of eq 6 above, and thus, we arrive at an approximate expression for E_q

$$E_{q,\text{nondipolar}} \cong K \frac{Q^2 \rho_q}{\sigma^2} r_{0s}^{-4/3} \quad (8)$$

Equation 8 expresses the contribution of the dipole solute–quadrupole solvent interaction to the stabilization energy.

MV theory is derived under the assumption that the solvent molecules are ideal, axially symmetric quadrupoles, and can only be properly applied to solvents with nearly axial symmetry.⁸⁶ Among the solvents we have examined, this effective axial approximation is applicable for ethylene, carbon dioxide, benzene, and toluene. We have also studied 1,2,4,5-tetrafluorobenzene (TFB) and dioxane, two solvents that cannot be approximated as axially symmetric, for contrast. Figure 6 exhibits a plot of excess stabilization energy versus $Q^2 \sigma^{-2} r_{0s}^{-4/3}$. Three comments are in order regarding this plot. First, it demonstrates a linear relationship for the axially symmetric solvents indicating a linear correlation between ADMA SH peak energy and Q^2 . This result is consistent with the MV prediction and helps to corroborate that validity of this theory. Second, TFB and dioxane do not fall on the line, suggesting a failure of MV theory for nonaxially symmetric quadrupolar solvents, a result that is not unexpected. Finally, the density factor has been omitted from the quantity against which the peak energy has been plotted. In our original paper, we indicated that inclusion of the density reduces the goodness of fit between these quantities and we speculated that this may reflect an unusual density dependence because the short range of dipole–quadrupole interactions. However, we have recently come to appreciate the fact that the approximate expressions in eqs 7 and 8 are derived within the condition that $R_0 \gg \sigma$, and therefore, variations in solvent size may affect the quality of the correlation between peak energy and $Q^2 \rho_q \sigma^{-2} r_{0s}^{-4/3}$. We intend to explore the density dependence of the quadrupolar solvation energy in future work through studies of ADMA in high-pressure quadrupolar fluids. Note, however, that the correlation between the excess solvation energy and Q^2 offers experimental evidence to establish the significance of the CO₂ quadrupole in solvating dipolar solutes such as the SH charge-transfer state of ADMA.

Spectroscopy of ADMA in Supercritical CO₂. The above results offer important insight into spectroscopic studies of solvation in supercritical CO₂. We note that the ADMA SH peak energies measured in SCF ethylene (solvent 12) and fluoroform (solvent 13) conform closely to expectations based on dielectric continuum models of solvation, whereas CO₂ exhibits a significant deviation from this model. These results indicate that the compressible nature of the solvent is not responsible for the excess peak shift in supercritical CO₂, but rather the excess shift arises from quadrupolar solvent interactions with a dipolar solute. Thus, we have demonstrated that an observation that is often associated with local density augmentation in SCFs is actually the result of solvent–solute interactions that exceed the predictions of the dielectric continuum model. Our analysis demonstrates that CO₂ behaves as a quintessentially quadrupolar solvent and highlights the fact that the large quadrupole moment of CO₂ coupled to its small size is responsible for its remarkable solvation properties.

V.B. Kinetics of the ADMA Charge-Transfer Reaction. *Supercritical CO₂.* Having demonstrated the importance of quadrupolar solvation for the ADMA SH state, we are now well-poised to examine the kinetics of the intramolecular charge-transfer reaction in SCF CO₂. In 1982, Eisenthal and co-workers had shown that the ADMA charge-transfer reaction exhibited a power law dependence on solvent viscosity in nonpolar solvents.⁷⁰ This observation was consistent with the chain

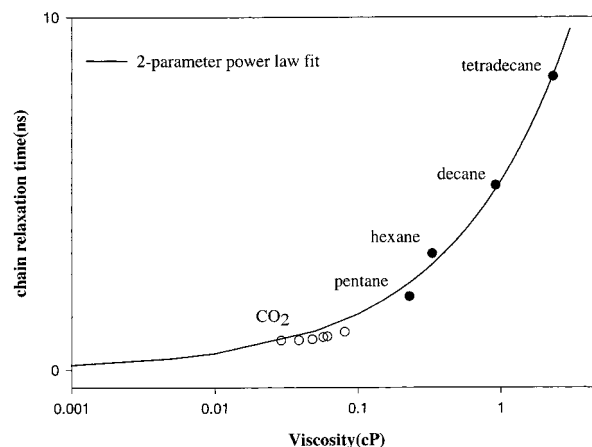


Figure 7. ADMA chain relaxation time vs logarithm of the bulk solvent viscosity. The closed circles are the experimental points including liquid data from ref 70 and SCF CO₂ data from ref 77. The line is a fit of the liquid data to a viscosity power law and indicates that the charge-transfer rate of ADMA in supercritical CO₂ is well characterized by the bulk viscosity. The observed isomerization rate is slightly faster than the prediction based on bulk CO₂ viscosity.

relaxation mechanism that was postulated for the reaction in nonpolar solvents. Late in 1998, we published a paper aimed at probing the influence of local density augmentation on the kinetics of this reaction resulting from fluid clustering of CO₂ around the nonpolar ground state of ADMA.⁷⁷ If fluid clustering around ADMA in the ground state resulted in a substantial increase in local viscosity, we expected to observe a reduction in the ADMA charge-transfer isomerization rate. Furthermore, if the quadrupole moment of CO₂ could support the long-range charge-transfer intermediate, we might also observe evidence for the polar mechanism (i.e., multiexponential fluorescence decays) in studies of the kinetics of this reaction. The results of our study demonstrated that the ADMA charge-transfer isomerization proceeds through the nonpolar mechanism in supercritical CO₂, indicating that its quadrupole moment is incapable of supporting an extended charge-transfer intermediate. Furthermore, the rate of the isomerization reaction was consistent with Eisenthal's viscosity power law prediction within the uncertainty of both sets of measurements. This result is illustrated in Figure 7. Note that the CO₂ rates exhibit a monotonic increase with increasing density and become faster than the viscosity power law prediction as the fluid density is increased, though the deviation from the prediction is small. This figure demonstrates that kinetic effects resulting from local solvent density augmentation are not observed for the ADMA charge-transfer isomerization, even though this reaction involves a large amplitude motion and is viscosity dependent. We also note that this solute is substantially larger than the diphenylpolyenes whose reactivity we have also studied in supercritical CO₂. The observed absence of local density enhancement in this case is consistent with the conclusions of the diphenylpolyene study, namely, that in the absence of strong solvent–solute interactions the bulk fluid viscosity adequately represents the environment experienced by the reactive solute molecule over the reaction time scale. (Importantly, this experiment only probes local density augmentation that occurs around the nonpolar ADMA LE state because the transition of individual ADMA molecules from nonpolar to polar is instantaneous. We are currently exploring dynamic aspects of charge-transfer state solvation, particularly in mixed solvent systems.⁷⁶) These results are consistent with the emerging view of the influence of SCF clustering on chemical kinetics discussed in sections II–IV.

Transition from the Nonpolar to Polar Mechanism. Recently we have begun to examine the kinetics of the ADMA isomerization reaction in a broad range of fluids spanning the intermediate polarity range. Although ADMA isomerization has been studied in both polar and nonpolar environments, the transition from nonpolar to polar solvents, and therefore the transition between nonpolar and polar mechanisms, has not been explored in a well-controlled fashion. Our recent results indicate two important features that deserve mention here. First, the transition from the nonpolar mechanism, characterized by a single exponential decay of the 420 nm fluorescence, to the polar mechanism, characterized by a multiexponential decay, occurs at a dielectric constant of about 5.5. Interestingly, dioxane, a liquid with a large quadrupole moment but a dielectric constant of only 2.2, appears to support the polar mechanism. We believe that this occurs not only because of the quadrupolar charge distribution but because dioxane can communicate its polar nature over relatively long spatial extent. Whether this occurs as a result of the large charge separation in dioxane itself or as a result of relatively strong intermolecular interactions between dioxane molecules is still an open question. This observation is particularly interesting in the context of the "dioxane anomaly", which has been the subjects of speculation for many years.^{87–89} The kinetics of ADMA charge-transfer isomerization offer a new and unique avenue for the examination of this anomalous behavior, and a manuscript on this phenomenon is in preparation. Second, our examination of the nonpolar mechanism across a range of solvents up to about $\epsilon = 5$ indicates that the rate of the nonpolar reaction deviates from the prediction based on Eyring's viscosity power law in a manner that exhibits a linear correlation with the solvatochromic peak shift observed in the SH emission peak. This observation has been made for nonpolar as well as quadrupolar solvents and indicates clearly that the nonpolar mechanism is influenced by solvent polarity. This implies that the nonpolar ADMA mechanism is not strictly diffusion-controlled. It appears to be an activated process with a polar transition state, and it seems likely that the activation barrier will be governed by solvent reorganization. Importantly, supercritical CO₂ can accelerate this reaction, indicating that its quadrupole moment offers sufficient "polarity" to influence a charge-transfer reaction. We are currently investigating these features of the ADMA reaction.

VI. Conclusions and Future Directions

On the basis of our studies of solvation and reactivity in a range of complex environments, and in the context of the results of numerous other researchers studying solvation and reactivity in SCF solvents, we have arrived at some general conclusions concerning the local environment around solutes in supercritical solvents. Solutes tend to find themselves in regions of high solvent density when they are dissolved in compressible supercritical solvents. Though this implies the clustering of fluid around the solute, it is also clear that solvent–solute interactions that influence solute spectroscopic observables are distinct from the long-range correlations that are the hallmark of critical phenomena in SCFs. Strong solvent–solute interactions influence spectroscopic observables such as solvatochromic shifts, rotational diffusion times, and unimolecular reaction rates, but these do not necessarily reflect condensation of the solvent around the solute. Rather, they arise as a result of the high sensitivity of these observables to electrostatic effects that can often be attributed to a small increase in the number of solvent molecules in the first one or two solvation shells around a solute molecule.

The influence of the local solvent environment on solvation and reactivity in SCF solvents has turned out to be more subtle than originally expected. Furthermore, in measuring such phenomena, it is often difficult to separate influences that are associated with compressible solvents from electrostatic and other influences that are simply not well characterized experimentally or theoretically. For example, our rotational diffusion studies have demonstrated that diphenylpolyenes exhibit nearly inertial rotational behavior across most of the compressible regime, whether or not strong solvent–solute interactions are at play. This has indicated to us that SCF solutions offer a fertile ground for the study of the transition from inertial rotation to diffusion-controlled rotation of molecules in solution.

Quadrupolar effects in dilute SCF solutions have only recently begun to yield to experimental examination, but it appears that these influences play a role in local density enhancement and contribute significantly to the observed kinetic acceleration of reactions. There is some controversy regarding the proper interpretation of diphenylpolyene kinetics in supercritical CO₂. However our studies of ADMA are unambiguous. Quadrupolar effects are responsible for a significant fraction of the solvation free energy of the ADMA exciplex in supercritical CO₂. Because we have demonstrated that the ADMA exciplex behaves as an ideal dipolar solute in a variety of solvents we have confidence that our conclusions regarding the importance of quadrupolar effects in solvation and reactivity of this solute will be generalized to a broad range of solutes. We have also established the importance of quadrupolar solvent–dipolar solute interactions in the charge-transfer reactivity of ADMA. This fact is consistent with the notion that quadrupolar solvent effects can accelerate the rates of diphenylpolyene isomerization reactions. Several recent experimental and theoretical investigations by other groups have begun to identify quadrupolar solvent–dipolar solute interactions as an important class of solvent effect in solvation and chemical reactivity, particularly in charge-transfer reactions.^{78–80,82,89} It appears that quadrupolar solvent effects on solvation and reactivity will receive increasing attention in the future.

Acknowledgment. It is my pleasure to acknowledge the diligent contributions of Mazdak Khajehpour, Kathy Wiemers, and Dr. Bob Anderton in these investigations. This work has been supported by the National Science Foundation, the Petroleum Research Fund, and the University of Missouri Research Board.

References and Notes

- (1) *Supercritical fluid cleaning: fundamentals, technology and applications*; McHardy, J., Sawan, S. P., Eds.; Noyes Publications: Westwood, NJ, 1998.
- (2) *Supercritical fluid engineering science: fundamentals and applications*; Kiran, E., Brennecke, J. F., Eds.; American Chemical Society: Washington, DC, 1993.
- (3) *Supercritical Fluid Technology: Theoretical and Applied Approaches in Analytical Chemistry*; Bright, F. V., McNally, M. E. P., Eds.; American Chemical Society: Washington, DC, 1992; Vol. 488.
- (4) Kajimoto, O. *Chem. Rev.* **1999**, *99*, 355.
- (5) Tucker, S. C. *Chem. Rev.* **1999**, *391*, 1.
- (6) Brennecke, J. F.; Chateaufneuf, J. E. *Chem. Rev.* **1999**, *99*, 433.
- (7) Eckert, C. A.; Ziger, D. H.; Johnston, K. P.; Kim, S. *J. Phys. Chem.* **1986**, *90*, 2738.
- (8) Smith, R. D.; Frey, S. L.; Yonker, C. R.; Gale, R. W. *J. Phys. Chem.* **1987**, *91*, 3059.
- (9) Yonker, C. R.; Smith, R. D. *J. Phys. Chem.* **1988**, *92*, 235.
- (10) Kim, S.; Johnston, K. P. *Ind. Eng. Chem. Res.* **1987**, *26*, 1206.
- (11) Betts, T. A.; Zagrobelny, J.; Bright, F. V. *J. Supercrit. Fluids* **1992**, *5*, 48.
- (12) Brennecke, J. F. *ACS Symp. Ser.* **1993**, *514*, 201.
- (13) Eckert, C. A.; Knutson, B. L. *Fluid Phase Equilib.* **1993**, *83*, 93.

- (14) Kajimoto, O.; Futakami, M.; Kobayashi, T.; Yamasaki, K. *J. Phys. Chem.* **1988**, *92*, 1347.
- (15) Kauffman, J. F. *Anal. Chem.* **1996**, *68*, 248A.
- (16) Morita, A.; Kajimoto, O. *J. Phys. Chem.* **1990**, *94*, 6420.
- (17) Sun, Y. P.; Fox, M. A.; Johnston, K. P. *J. Am. Chem. Soc.* **1992**, *114*, 1187.
- (18) Chialvo, A. A.; Cummings, P. T. *AIChE J.* **1994**, *40*, 1558.
- (19) Egorov, S. A.; Yethiraj, A.; Skinner, J. L. *Chem. Phys. Lett.* **2000**, *317*, 558.
- (20) Martinez, H. L.; Ravi, R.; Tucker, S. C. *J. Chem. Phys.* **1996**, *104*, 1067.
- (21) Tucker, S. C.; Maddox, M. W. *J. Phys. Chem. B* **1998**, *102*, 2437.
- (22) Ruckenstein, E.; Shulgin, I. L. *Chem. Phys. Lett.* **2000**, *330*, 551.
- (23) Luo, H.; Tucker, S. C. *Theor. Chem. Acc.* **1997**, *96*, 84.
- (24) Adams, J. E. *J. Phys. Chem. B* **1998**, *102*, 7455.
- (25) Urdahl, R. S.; Myers, D. J.; Rector, K. D.; Davis, P. H.; Cherayil, B. J.; Fayer, M. D. *J. Chem. Phys.* **1997**, *107*, 3747.
- (26) Cherayil, B. J.; Fayer, M. D. *J. Chem. Phys.* **1997**, *107*, 7642.
- (27) Myers, D. J.; Shigeiwa, M.; Stromberg, C.; Fayer, M. D.; Cherayil, B. *J. Chem. Phys. Lett.* **2000**, *325*, 619.
- (28) Egorov, S. A.; Skinner, J. L. *J. Chem. Phys.* **2000**, *112*, 275.
- (29) Goodyear, G.; Tucker, S. C. *J. Chem. Phys.* **1999**, *110*, 3643.
- (30) Anderton, R. M.; Kauffman, J. F. *J. Phys. Chem.* **1995**, *99*, 13759.
- (31) Bauer, D. R.; Brauman, J. I.; Pecora, R. *J. Am. Chem. Soc.* **1974**, *96*, 6840.
- (32) Betts, T. A.; Zagrobelny, J.; Bright, F. V. *J. Am. Chem. Soc.* **1992**, *114*, 8163.
- (33) Heitz, M. P.; Bright, F. V. *J. Phys. Chem.* **1996**, *100*, 6889.
- (34) Heitz, M. P.; Maroncelli, M. *J. Phys. Chem.* **1997**, *101*, 5852.
- (35) Dote, J. L.; Kivelson, D.; Schwartz, R. N. *J. Phys. Chem.* **1981**, *85*, 2169.
- (36) Kauffman, J. F.; Wiemers, K.; Khajehpour, M. *Rev. High Pres. Sci. Technol.* **1998**, *7*, 1225.
- (37) Wiemers, K. L.; Kauffman, J. F. *J. Phys. Chem.* **2000**, *104A*, 451.
- (38) Nee, T.-W.; Zwanzig, R. *J. Chem. Phys.* **1970**, *52*, 6353.
- (39) Dutt, G. B.; Srivatsavoy, V. J. P.; Sapre, A. V. *J. Chem. Phys.* **1999**, *110*, 9623.
- (40) Srinivas, G.; Bhattacharyya, S.; Bagchi, B. *J. Chem. Phys.* **1999**, *110*, 4477.
- (41) Hubbard, J. B.; Wolynes, P. G. *J. Chem. Phys.* **1978**, *69*, 998.
- (42) Alavi, D. S.; Waldeck, D. H. *J. Chem. Phys.* **1991**, *94*, 6196.
- (43) Kumar, P. V.; Maroncelli, M. *J. Chem. Phys.* **2000**, *112*, 5370.
- (44) Kurnikova, M. G.; Balabai, N.; Waldeck, D. H.; Coalson, R. D. *J. Am. Chem. Soc.* **1998**, *120*, 6121.
- (45) Kurnikova, M. G.; Waldeck, D. H.; Coalson, R. D. *J. Chem. Phys.* **1996**, *105*, 628.
- (46) Brey, L. A.; Schuster, G. B.; Drickamer, H. G. *J. Chem. Phys.* **1979**, *71*, 2765.
- (47) Andrews, J. R.; Hudson, B. S. *J. Chem. Phys.* **1978**, *68*, 4587.
- (48) Velsko, S. P.; Waldeck, D. H.; Fleming, G. R. *J. Chem. Phys.* **1983**, *78*, 249.
- (49) Anderton, R. M.; Kauffman, J. F. *J. Phys. Chem.* **1994**, *98*, 12125.
- (50) Anderton, R. M.; Kauffman, J. F. *J. Phys. Chem.* **1995**, *99*, 14628.
- (51) Gehrke, C.; Schroeder, J.; Schwarzer, D.; Troe, J.; Vob, F. *J. Chem. Phys.* **1990**, *92*, 4805.
- (52) Keery, K. M.; Fleming, G. R. *Chem. Phys. Lett.* **1982**, *93*, 322.
- (53) Schroeder, J.; Schwarzer, D.; Troe, J. *Ber. Bunsen-Ges. Phys. Chem.* **1990**, *94*, 1249.
- (54) Schroeder, J. *Ber. Bunsen-Ges. Phys. Chem.* **1991**, *95*, 233.
- (55) Wiemers, K. L.; Kauffman, J. F. *J. Phys. Chem. A* **2001**, *105*, 823.
- (56) Kramers, H. A. *Physica* **1940**, *7*, 284.
- (57) Sun, Y. P.; Saltiel, J. *J. Phys. Chem.* **1989**, *93*, 8310.
- (58) Lee, M.; Bain, A. J.; McCarthy, P. J.; Han, C. H.; Haseltine, J. N.; Smith, A. B., III.; Hochstrasser, R. M. *J. Chem. Phys.* **1986**, *85*, 4341.
- (59) Hubbard, P. S. *Phys. Rev.* **1963**, *131*, 1155.
- (60) Grote, R. F.; Hynes, J. T. *J. Chem. Phys.* **1980**, *73*, 2715.
- (61) Schroeder, J.; Schwarzer, D.; Troe, J.; Vob, F. *J. Chem. Phys.* **1990**, *93*, 2393.
- (62) Gehrke, C.; Mohrschladt, R.; Schroeder, J.; Troe, J.; Vohringer, P. *Chem. Phys.* **1991**, *152*, 45.
- (63) Schroeder, J.; Schwarzer, D.; Troe, J.; Vohringer, P. *Chem. Phys. Lett.* **1994**, *218*, 43.
- (64) Velsko, S. P.; Fleming, G. R. *J. Chem. Phys.* **1982**, *76*, 7335.
- (65) Courtney, S. H.; Fleming, G. R. *Chem. Phys. Lett.* **1984**, *103*, 443.
- (66) Anderton, R. M.; Kauffman, J. F. *Chem. Phys. Lett.* **1995**, *237*, 145.
- (67) Zhang, J.; Roek, D. P.; Chateaufeuf, J. E.; Brennecke, J. F. *J. Am. Chem. Soc.* **1997**, *119*, 9980.
- (68) Chuang, T. J.; Cox, R. J.; Eisenthal, K. B. *J. Am. Chem. Soc.* **1974**, *96*, 6828.
- (69) Crawford, M. K.; Wang, Y.; Eisenthal, K. B. *Chem. Phys. Lett.* **1981**, *79*, 529.
- (70) Wang, Y.; Crawford, M. C.; Eisenthal, K. B. *J. Am. Chem. Soc.* **1982**, *104*, 5874.
- (71) Masaki, S.; Okada, T.; Mataga, N.; Sakata, Y.; Misumi, S. *Bull. Chem. Soc. Jpn.* **1976**, *44*, 1277.
- (72) Migita, M.; Okada, T.; Mataga, N.; Nakashima, N.; Yoshihara, K.; Sakata, Y.; Misumi, S. *Bull. Chem. Soc. Jpn.* **1981**, *54*, 3304.
- (73) Okada, T.; Migita, M.; Mataga, N.; Sakata, Y.; Misumi, S. *J. Am. Chem. Soc.* **1981**, *103*, 4715.
- (74) Hirata, Y.; Kanda, Y.; Mataga, N. *J. Phys. Chem.* **1983**, *87*, 1659.
- (75) Hui, M.-H.; Ware, W. R. *J. Am. Chem. Soc.* **1976**, *98*, 4718.
- (76) Khajehpour, M.; Kauffman, J. F. *J. Phys. Chem. A* **2000**, *104*, 7151.
- (77) Khajehpour, M.; Kauffman, J. F. *Chem. Phys. Lett.* **1998**, *297*, 141.
- (78) Reynolds, L.; Gardecki, J. A.; Frankland, S. J. V.; Horng, M. L.; Maroncelli, M. *J. Phys. Chem.* **1996**, *100*, 10337.
- (79) Matyushov, D. M.; Voth, G. A. *J. Chem. Phys.* **1999**, *111*, 3630.
- (80) Vath, P.; Zimmt, M. B.; Matyushov, D. V.; Voth, G. A. *J. Phys. Chem. B* **1999**, *103*, 9130.
- (81) Vath, P.; Zimmt, M. B. *J. Phys. Chem. A* **2000**, *104*, 2626.
- (82) Read, I.; Napper, A.; Zimmt, M. B.; Waldeck, D. H. *J. Phys. Chem. A* **2000**, *104*, 9385.
- (83) Syage, J. A.; Felker, P. M.; Zewail, A. H. *J. Chem. Phys.* **1984**, *81*, 2233.
- (84) Kajimoto, O.; Hayami, S.; Shizuka, H. *Chem. Phys. Lett.* **1991**, *177*, 219.
- (85) Mataga, N.; Kubota, T. *Molecular Interactions and Electronic Spectra*; Marcel Dekker: New York, 1970.
- (86) Khajehpour, M.; Kauffman, J. F. *J. Phys. Chem. A* **2000**, *104*, 9512.
- (87) Ledger, M. B.; Suppan, P. *Spectrochim. Acta A* **1967**, *23*, 3007.
- (88) Suppan, P. *J. Photochemistry* **1982**, *18*, 289.
- (89) Geerlings, J. D.; Varna, C. A. G. O.; Hemmert, M. C. v. *J. Phys. Chem. B* **2000**, *104*, 56.